

# Electrical and Optical Properties of an Organic Semiconductor Based on Polyaniline Prepared by Emulsion Polymerization and Fabrication of Ag/Polyaniline/n-Si Schottky Diode

F. Yakuphanoglu,<sup>\*,†</sup> E. Basaran,<sup>‡</sup> B. F. Şenkal,<sup>§</sup> and E. Sezer<sup>§</sup>

Department of Physics, Faculty of Arts and Sciences, Firat University, 23119 Elazığ, Turkey, Department of Physics, Gebze Institute of Technology, 41400, Gebze, Turkey, and Department of Chemistry, Faculty of Arts and Sciences, İstanbul Technical University, Maslak, İstanbul, Turkey

Received: January 21, 2006; In Final Form: May 25, 2006

The electrical, optical, and metal–semiconductor contact properties of the polyaniline prepared by emulsion polymerization have been investigated to obtain an organic semiconductor material. The obtained results suggest that the polyaniline (PANI) studied is an organic semiconductor material with optical band gap ( $E_g = 2.21$  eV) and room electrical conductivity ( $\sigma_{25} = 3.12 \times 10^{-2}$  S/cm) values. A Schottky diode with configuration Ag/PANI/n-Si was fabricated. The ideality factor and barrier height of Ag/PANI/n-Si diode at room temperature were found to be 4.59 and 0.38 eV, respectively. The obtained diode parameters change with temperature. The Richardson constant  $A^*$  value for the Ag/PANI/n-Si diode was found to be  $3.81 \times 10^{-4}$  A/cm<sup>2</sup>·K. The Ag/PANI/n-Si diode is a metal–insulator–semiconductor-type device. The standard deviation, which is a measure of the barrier homogeneity, was found to be 0.14, indicating the presence of interface inhomogeneities. It can be concluded that the polyaniline prepared by emulsion polymerization is an organic semiconductor and Ag/PANI/n-Si configuration shows a Schottky contact.

## 1. Introduction

Electrical conduction in macromolecular systems is an interesting research field, from both theoretical and experimental points of view. The conjugated polymers exhibit conducting or semiconducting properties. Semiconducting polymers are now attracting considerable attention as promising materials for the development of optoelectronic devices such as light-emitting diodes, photovoltaic cells, and nonlinear optical systems.<sup>1–6</sup> Recent attention in the field of polymer science has been paid to conjugated polymers, due to their characteristic optical, electrical, and magnetic properties.<sup>7</sup> Polyaniline is a polymer with an outstanding thermal stability, in air, which has electrical features ranging from an insulator to a metallic state, depending on the oxidation state and dopant.<sup>8</sup> Organic semiconductor polymers with metals have been used to fabricate Schottky barriers. This has opened a new possibility of replacing conventional inorganic devices by organic ones. Polyaniline is known as a p-type semiconductor.<sup>9</sup> The fabrication of polyaniline-based microelectronics devices such as Schottky diodes has been reported.<sup>10–12</sup>

The aim of this study is to investigate the electrical and optical properties of polyaniline prepared by emulsion polymerization to obtain the organic semiconductor and to fabricate organic semiconductor–metal Schottky contact.

## 2. Experimental Section

**2.1. Preparation of Polymeric Surfactant.** The polymeric surfactant was prepared (Scheme 1) in two steps starting from polyglycidyl methacrylate as follows:

*Modification of PolyGMA with Diethylamine.* Polyglycidyl methacrylate (polyGMA;  $M_n = 43\,000$ ) (8 g) was dissolved in 2-methyl-1-pyrrolidone (30 mL) and then this solution was put in 25 mL of diethylamine in a 100 mL flask. The mixture was stirred for 24 h at room temperature. While stirring, it was heated at 80 °C in a thermostated oil bath for 3 h. After it was chilled, the mixture was poured into 250 mL of distilled water, washed with excess water (1 L) and with 25 mL of alcohol, and dried overnight under vacuum for 24 h. The yield was 9.3 g.

*Quaternization of Aminated PolyGMA with Chloroacetone.* Aminated polyGMA (5 g) was dissolved in 2-methyl-1-pyrrolidone (20 mL), and chloroacetone (3 g, 32.43 mmol) was placed in this solution. The mixture was stirred for 3 days at room temperature. After reaction, the mixture was poured into diethyl ether. The precipitated polymer was filtered and washed with ether. The product was dried under vacuum at room temperature for 24 h.

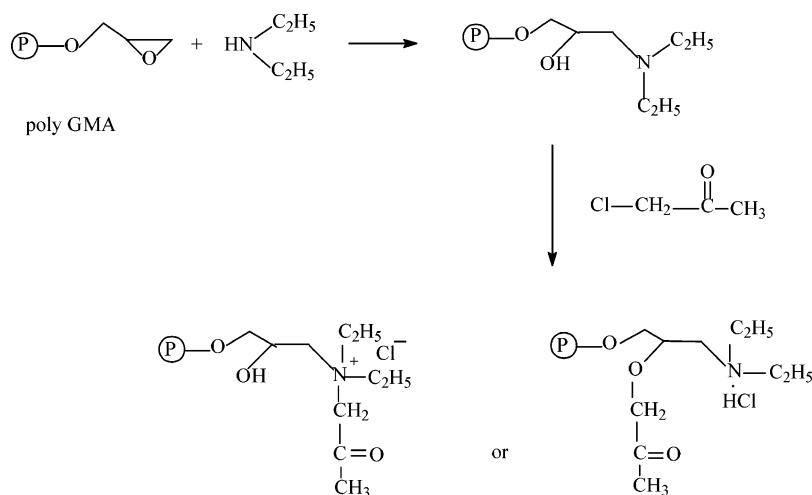
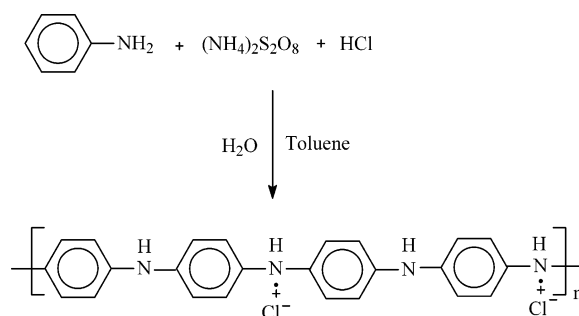
In the Fourier transform infrared (FTIR) spectra of starting compound, the C–O stretching vibration band of the CH–OH group becomes weak after reaction. This can be ascribed to ether formation during quaternization.

**2.2. Emulsion Polymerization of Aniline in the Presence of Polymeric Surfactant.** Polyaniline (PANI) was synthesized by the chemical oxidation of aniline with ammonium persulfate as oxidant. Aniline (1.0 g, 0.011 mol) in 25 mL of toluene was added in 200 mL of the surfactant-containing water (0.04 g/200 mL). To this solution, 3.42 g (0.015 mol) of ammonium persulfate solution in 50 mL of 1 M HCl was added dropwise while stirring. The reaction was continued for 1 h at 0 °C and then for 24 h at room temperature. After this time, no precipitation was observed. The reaction mixture was poured into 200 mL of aqueous NaOH solution (1 M). The polymer precipitated was filtered and washed with excess water to

<sup>†</sup> Firat University.

<sup>‡</sup> Gebze Institute of Technology.

<sup>§</sup> İstanbul Technical University.

**SCHEME 1: Preparation of Polymeric Surfactant****SCHEME 2: Soluble Emeraldine Salt**

remove soluble fractions. The filtered cake was then dried under vacuum for 24 h. The reaction mechanism is depicted in Scheme 2.

Characterization of the resulting polymer was performed by FTIR—attenuated total reflectance (ATR) measurements. Characteristic peaks of PANI observed in the FTIR spectra (Figure 1) of polymer are summarized in Table 1, and they are in agreement with literature.<sup>13</sup>

**2.3. Measurements and Fabrication of the Schottky Diode.**

The substrate used in this study is n-Si(100). The native oxide on the front surface of the substrate was removed in HF/H<sub>2</sub>O solution, then was rinsed in deionized water by use of an ultrasonic bath for 20 min, and finally was chemically cleaned by baths of methanol and acetone.

Cyclic voltammetry was conducted with a Parstat 2263 model potentiostat—galvanostat. A standard three-electrode configuration cell was used for the electrochemical analysis with 1 M HCl. An n-Si electrode (area 0.50 cm<sup>2</sup>) was used as working electrode; it was rinsed thoroughly with ethanol and acetone. Pt and Ag wires were used as counterelectrode and quasi-reference electrode, respectively. Potentials versus the Ag quasi-reference electrode were then rescaled versus Ag/AgCl calibrated with the ferrocene/ferrocenium redox couple (0.35 V vs Ag/AgCl). Monomer solutions were prepared at concentration about 1.0 mM. Electrochemical polymerization of monomers was performed at ambient temperature under potentiodynamic conditions in the range of −0.2 to 1.2 V. After the polymerization process, the polymer-coated Si was cleaned by methanol

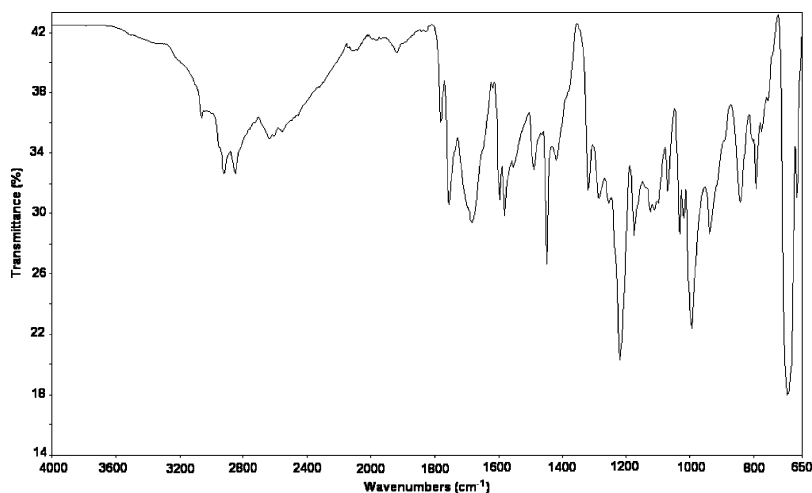


**Figure 1.** FTIR spectra of PANI obtained by emulsion polymerization.

TABLE 1: Characteristic Peaks of PANI

peak <sup>a</sup>	assignments
1288–1214	-C–N stretching
1228–1221	-C–N <sup>+</sup> stretching
1522–1480	-C=N stretching
1401–1383	-C=N <sup>+</sup> stretching
1625–1615 (B), 1580–1590 (Q)	aromatic ring
1185–1175 (B), 1160–1180 (Q)	-CH (ip) (inner plane bending)
822–810 (B), 780–800 (Q)	-CH (op) (outer plane bending)
1540–1495 (B), 1540–1570 (Q)	ring stretching
1315–1285 (B), 1290–1300 (Q)	-CN stretching

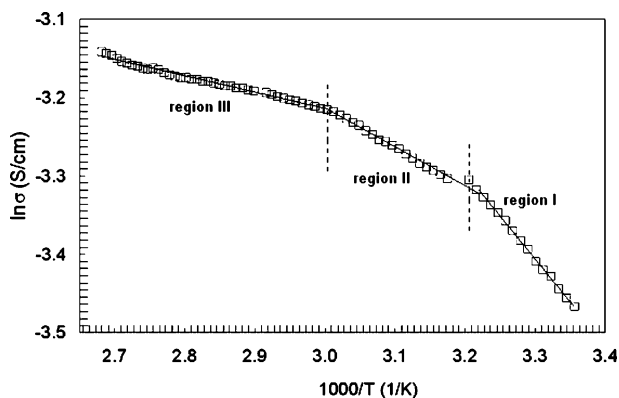
<sup>a</sup> B, benzonoid; Q, quinoid.

Figure 2. Conductivity dependence on temperature of the PANI.

at room temperature. The Ag metal was deposited onto the PANI organic film by vacuum evaporation. The diode contact area was found to be  $7.85 \times 10^{-3} \text{ cm}^2$ . Temperature dependence of direct current electrical conductivity (DC) of the sample was performed by employing a Keithley 6517A electrometer under dark conditions and normal atmospheric medium in a furnace with a heating rate of  $4 \text{ }^\circ\text{C/min}$ . The current–voltage characteristics of the Ag/PANI/n-Si diode were measured on a Keithley 6517A electrometer. To measure the optical absorption, the PANI was prepared as a thin pellet so that UV–visible beam can pass through the PANI. UV spectra of the polymer were recorded at room temperature with a Shimadzu 1240 spectrophotometer.

### 3. Results and Discussion

**3.1. Electrical Conductivity of Polyaniline (PANI) Prepared by Emulsion Polymerization.** The temperature dependence of the conductivity of the polyaniline prepared by emulsion is shown in Figure 2. The conductivity versus  $1000/T$  curve shows three different straight lines (regions I, II, and III) with negative slopes. We believe that three types of conduction mechanism occur, one at the first conduction region (I), another at the second conduction region (II), and another at the third conduction region (III), as shown in Figure 2; that is, there is more than one charge transport mechanism in the PANI depending on the temperature range. The slope of conductivity regions can change widely depending on the nature and structure of the sample. The total conductivity of the PANI can be written as

$$\sigma(T) = \sigma_I \exp(-E_I/kT) + \sigma_{II} \exp(-E_{II}/kT) + \sigma_{III} \exp(-E_{III}/kT) \quad (1)$$

TABLE 2: Electronic Parameters of PANI

$E_I$ (meV)	$E_{II}$ (meV)	$E_{III}$ (meV)	$\sigma_I$ (S/cm)	$\sigma_{II}$ (S/cm)	$\sigma_{III}$ (S/cm)
93.04	45.22	17.88	1.17	0.19	0.075

where  $\sigma_I$ ,  $\sigma_{II}$ , and  $\sigma_{III}$  are constants and  $E_I$ ,  $E_{II}$ , and  $E_{III}$  are activation energies for each electrical conductivity region. These parameters were determined and are given in Table 2. The conductivity of the PANI increases steadily up to a certain temperature. The conductivity dependence of temperature does not obey the Arrhenius relationship in the temperature range from 25 to  $100 \text{ }^\circ\text{C}$ . A jump in the conductivity curve at  $T = 312.5 \text{ K}$  is observed. This jump in the conductivity can result from phase-transition-related structural and physical changes.<sup>14</sup> In region I, the electrical conductivity is thermally activated conductivity that obeys the Arrhenius formula, meaning that the conduction is due to thermal excitation of charge carriers. In region II, a deviation from the Arrhenius equation appears within the temperature range of 312–333 K, that is, the conductivity increases slowly, while in region III (333–373 K) it increases at a lower rate. In regions II and III, the conductivity is probably due to interchain and intrachain conductivities. The activation energy value for region III is lower than that of region II. It is evaluated that lower activation energy corresponds to interchain conductivity, while activation energy of the region is associated with intrachain conductivity. The electrical conductivity of PANI results from the conjugation of the main chain in the structure of the polymer. The voltage and heat applied will raise an electron from the atomic site to the another atomic site of main chain, that is, the  $\pi$ -electrons on the main chain of the polymer will be delocalized. The increase in conductivity of the PANI takes place by applied heat and voltage. In particular, the proportions of quinonoid imine ( $=\text{N}-$  moiety), benzenoid amine ( $-\text{NH}-$  moiety), and positively charged nitrogens corresponding to a particular oxidation and protonation level of the polymer can be quantitatively differentiated with proper curve-fitting. Fourier transform infrared (FTIR) spectroscopy and nonresonance FT–Raman spectroscopy have been used to measure qualitatively the various intrinsic oxidation states of PANI. Tang et al.<sup>15</sup> have assigned the  $1600 \text{ cm}^{-1}$  peak to the quinonoid ring and the  $1500 \text{ cm}^{-1}$  peak to the benzenoid ring. Furthermore, the IR absorption spectra of our polymer exhibit an enhanced quinonoid to benzenoid band intensity ratio (ratio is 1.19). This result indicates the presence of higher conjugation in PANI studied. The electrical conductivity results from conjugation with charge carrier traveling through the backbone of the polymer supplying sufficient voltage.<sup>16</sup> It is evaluated that the conjugation in the polymer is enough to make an organic semiconductor if it were present in the main chain of the polymer.

**3.2. Determination of the Optical Band Gap of the Polymer.** Figure 3 shows the absorption spectra of the PANI. The optical band gap energy of the PANI can be obtained from the relation given by<sup>17</sup>

$$\alpha h\nu = B(h\nu - E_g)^s \quad (2)$$

where  $B$  is an energy-independent constant and  $E_g$  is the optical band gap. This equation can be written as

$$\frac{d[\ln(\alpha h\nu)]}{d(h\nu)} = \frac{s}{h\nu - E_g} \quad (3)$$

When the value of  $s$  is determined, the type of transition can be obtained from the absorption spectrum. A discontinuity in

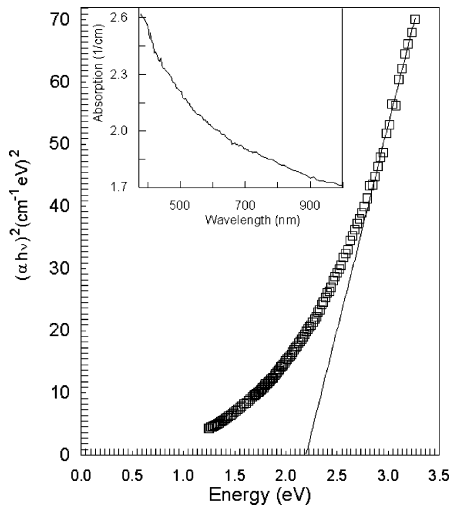


Figure 3. Plot of  $(\alpha h\nu)^2$  vs  $(h\nu)$  of PANI.

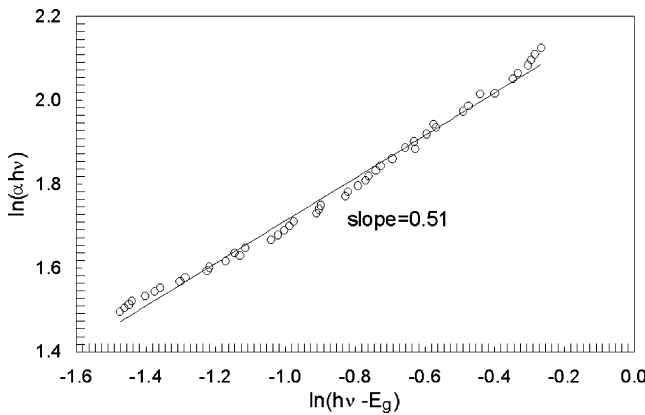


Figure 4. Plot of  $\ln(\alpha h\nu)$  vs  $\ln(h\nu - E_g)$  of PANI.

the  $d[\ln(\alpha h\nu)]/d(h\nu)$  versus  $h\nu$  plot at the band gap energy ( $E_g$ ), that is, at  $h\nu = E_g$ , can be observed. The discontinuity at a particular energy value gives the band gap,  $E_g$ . The curve of  $\ln(\alpha h\nu)$  versus  $\ln(h\nu - E_g)$  was plotted by use of the obtained  $E_g$  value, and the  $s$  value was found to be about  $1/2$  from the slope of the curve (Figure 4). Thus, we plotted  $(\alpha h\nu)^2$  versus  $h\nu$  to calculate a more precise value of the optical band gap. The optical band gap was determined by extrapolating the linear portion of the plot to  $(\alpha h\nu)^2 = 0$  (Figure 3).<sup>16,17</sup> This suggests that the fundamental absorption edge in the PANI is formed by the direct allowed transitions. The optical band gap of the polyaniline studied was compared with the optical band gap of pure polyaniline. The optical band gap of the polyaniline studied ( $E_g = 2.21$  eV) is lower than that of the polyaniline prepared by other methods ( $E_g = 3.04$  eV,<sup>18</sup>  $E_g = 3.65$  eV,<sup>19</sup> and  $E_g = 2.6$  eV<sup>20</sup>).

### 3.3. Fabrication of the Ag/PANI/n-Si Schottky Diode.

Figure 5 shows the forward and reverse bias  $I$ – $V$  characteristics of the Ag/PANI/n-Si at different temperatures. The standard thermoionic emission theory is used to obtain the characteristic parameters of the Schottky barrier devices.<sup>21,22</sup> The thermionic emission current can be described by the following relationship:<sup>21,22</sup>

$$I = I_0 \exp\left(\frac{qV}{nkT}\right) \left[1 - \exp\left(-\frac{qV}{nkT}\right)\right] \quad (4)$$

where  $I_0$  is the saturation current,  $T$  is the temperature,  $q$  is the electronic charge,  $k$  is the Boltzmann constant, and  $V$  is the

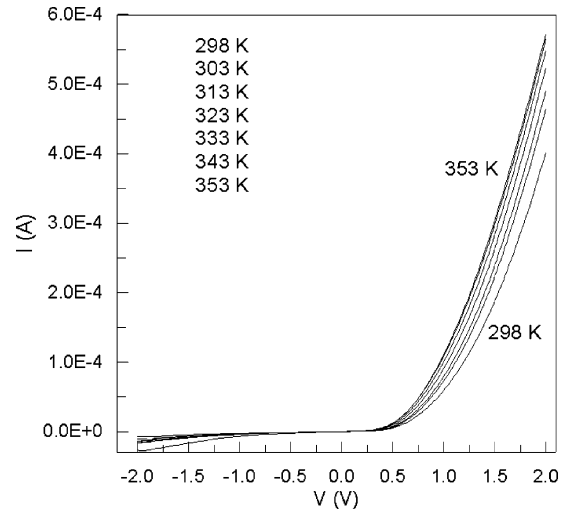


Figure 5.  $I$ – $V$  characteristics of the Ag/PANI/n-Si Schottky diode at different temperatures.

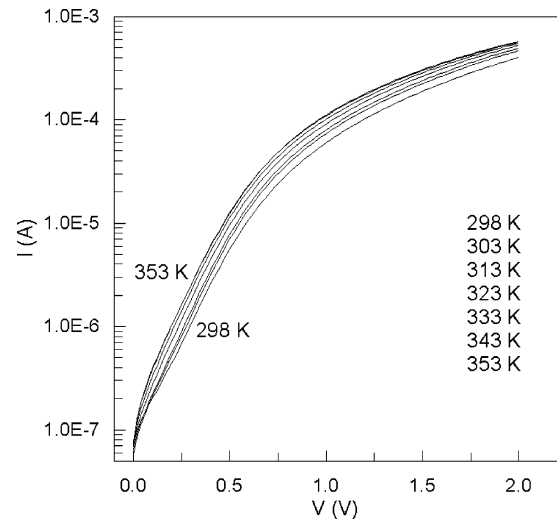


Figure 6. Forward current characteristics of the Ag/PANI/n-Si Schottky diode.

voltage. For bias voltages larger than  $3kT/q$ , the current as a function of applied voltage is expressed as<sup>23,24</sup>

$$I = I_0 \exp\left[\frac{qV}{nkT}\right] \quad (5)$$

where  $I_0$  is the saturation current and equals the  $\ln I$  intercept, and  $n$  is the ideality factor and it may be determined from the slope of the  $\ln I$ – $V$  graph. The  $n$  ideality factor, which is a measure of conformity of the diode to pure thermoionic emission, may be expressed by

$$n = \frac{q}{kT} \frac{dV}{d \ln I} \quad (6)$$

The value of the ideality factor,  $n$ , was calculated from the slope of the linear region of the forward  $\ln I$ – $V$  characteristics plotted in Figure 6 and is given in Table 3. This device is nonideal, showing a diode quality factor  $n > 1$ , that is, Ag/PANI/n-Si diode is a nonideal contact. The deviation from the ideal current–voltage characteristic of the diode is due to the presence of an interfacial layer and effect of series resistance. The obtained results indicate that the Ag/PANI/n-Si diode has a

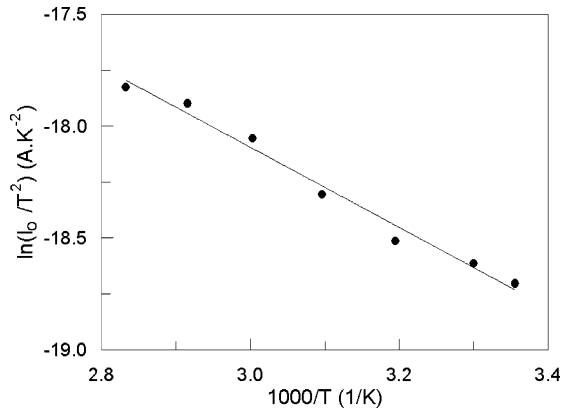


**Figure 7.** Plot of  $\ln(I_0/T^2)$  vs  $1000/T$  of the Ag/PANI/n-Si Schottky diode.

**TABLE 3: Electronic Parameters of Ag/PANI/n-type Si**

$T$ (K)	$n$	$\phi_B$ (eV)	$m$	$T_t$ (K)
298	4.59	0.38	3.41	718.76
303	4.39	0.39	3.40	728.11
313	4.30	0.40	3.36	738.74
323	4.11	0.41	3.28	737.41
333	4.10	0.42	3.21	735.59
343	3.97	0.43	3.18	748.42
353	3.94	0.44	3.17	768.83

metal–insulator–semiconductor configuration. The saturation current is given by the following relationship:<sup>21</sup>

$$I_0 = AA^*T^2 \exp\left(-\frac{q\phi_B}{kT}\right) \quad (7)$$

where  $\phi_B$  is the barrier height,  $A$  is the diode area, and  $A^*$  is the Richardson constant. The temperature dependence of  $I_0$  is shown in Figure 7. The  $A^*$  value was calculated from Figure 7 and was found to be  $3.81 \times 10^{-4}$  A/cm<sup>2</sup>·K. The values of the barrier height of diode were determined by use of the  $I_0$  values via eq 7 and are given in Table 3. The  $\phi_B$  values increase with increasing temperature.

**3.4. Space Charge Limited Current Mechanism of the Ag/PANI/n-Si Diode.** At higher voltages, a space charge injection can be proceed through the Ag/PANI/n-Si diode from the Ag metal to n-Si and organic layer, and in this case, the current is called the space charge limited current (SCLC).<sup>20</sup> Detailed information about the transport mechanism of the diode can be provided by current–voltage characteristics. The current–voltage curves at different temperatures are shown in Figure 8. It is observed that the current changes in the form of  $I \propto V^m$ .  $m$  values were calculated from the slope of Figure 8 and are given in Table 3. At lower voltages, the slope  $m$  of  $\ln I - \ln V$  plots is approximately unity, while at higher voltages, the slope changes between 3.41 and 3.17. The  $m$  values indicate that in the second region the carrier transport may be dominated by a space charge limited-conduction mechanism (SCLC),<sup>25</sup> where current increases superlinearly, that is,  $I \propto V^{m>2}$ , suggesting that the traps are exponentially distributed. The  $m$  value decreases with increasing temperature. This confirms a SCLC model controlled by an exponential distribution of traps. The power-law dependence between current and voltage is characterized by space charge limited currents. Therefore, the current is expressed as<sup>25</sup>

$$I = \frac{qA\mu N_V}{d^{l+1}} \left( \frac{\epsilon\epsilon_0}{eP_0kT_t} \right)^l V^{l+1} \quad (8)$$

where  $\epsilon$  is the dielectric constant of the semiconductor,  $e$  is the

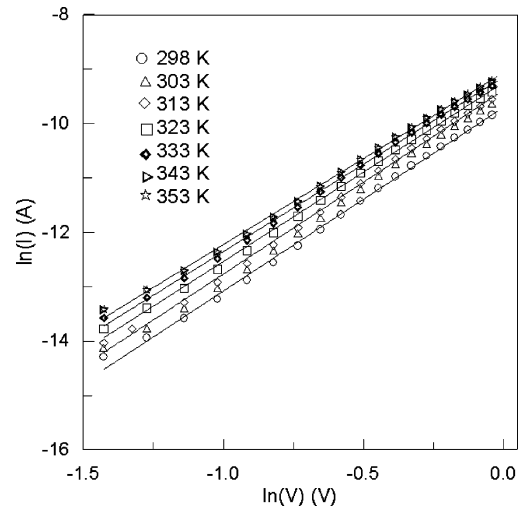


**Figure 8.** Plots of  $\ln I$  vs  $\ln V$  of the Ag/PANI/n-Si Schottky diode at different temperatures.

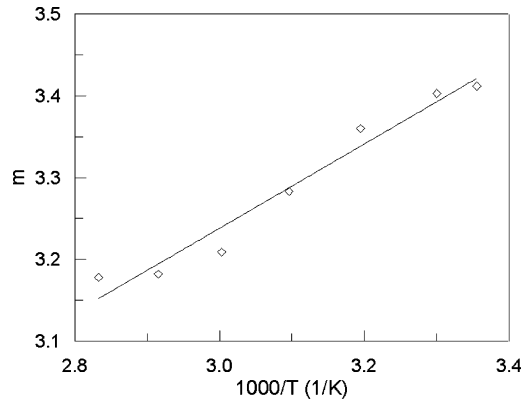


**Figure 9.** Plot of  $m$  versus  $1000/T$  of Ag/PANI/n-Si.

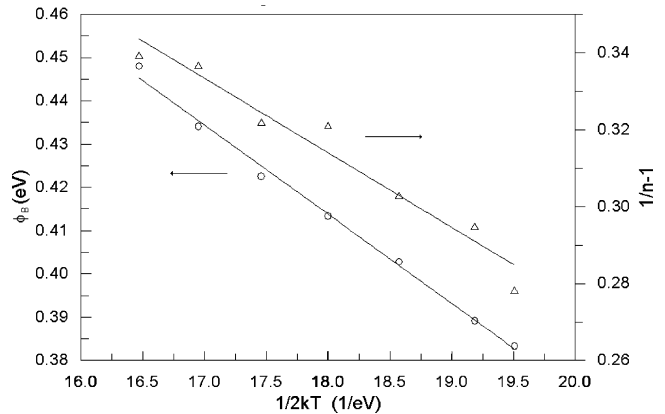


**Figure 10.** Plots of  $\phi_{ap}$  vs  $1/2kT$  and  $1/(n_{ap} - 1)$  vs  $1/2kT$  of the Ag/PANI/n-Si diode.

electronic charge,  $\mu$  is the mobility of carrier charges,  $N_V$  is the effective density of states in valence band edge,  $d$  is the thickness of the sample,  $l$  ( $l = m - 1$ ) is a parameter given by  $l = T_t/T$ , and  $T_t$  is a characteristic temperature of the exponential distribution of the traps.<sup>25</sup>  $T_t$  values were calculated and are given in Table 3. Figure 9 shows the dependence of  $m$  values on temperature. The exponential trap distribution can be expressed as

$$n = n_0 \exp\left(-\frac{E_t}{kT}\right) \quad (9)$$



where  $n$  is the trap concentration and total concentration is given as

$$N_t = n_0 kT_t \quad (10)$$

where  $kT_t = E_t$  is the characteristic energy of the exponential distribution of traps.  $E_t$  value was calculated from the slope of Figure 9 and was found to be 44.29 meV.

**3.5. Inhomogeneous Barrier Analysis.** A decrease in  $\phi_B$  and an increase in the ideality factor of the diode with decreasing temperature were observed. In some studies, this case has been successfully explained on the basis of a thermoionic mechanism with Gaussian distribution of barrier heights due to the barrier height inhomogeneities prevailing at the metal–semiconductor interface. The Gaussian distribution of the apparent barrier height and variation of the ideality factor with temperature are expressed by the following relationships:<sup>26–28</sup>

$$\phi_{ap} = \phi_{b0} - \frac{q\sigma_0^2}{2kT} \quad (11)$$

and

$$\left(\frac{1}{n_{ap}} - 1\right) = -\rho_2 + \frac{q\rho_3}{2kT} \quad (12)$$

where  $\phi_{ap}$  is the apparent barrier height,  $\sigma_0$  is the standard deviation of the barrier height distribution,  $n_{ap}$  is the apparent ideality factor, and  $\rho_2$  and  $\rho_3$  are the voltage deformation of the barrier height distribution. The plots of  $\phi_{ap}$  versus  $1/2kT$  and  $1/(n_{ap} - 1)$  versus  $1/2kT$  are in Figure 10. The standard deviation, which is a measure of the barrier homogeneity, was determined from the slope of  $\phi_{ap}$  versus  $1/2kT$  and it is found to be 0.14. This indicates the presence of interface inhomogeneities. The values of  $\rho_2$  and  $\rho_3$  were determined from the plot of  $1/(n_{ap} - 1)$  versus  $1/2kT$  and are found to be 0.66 and 0.019 V, respectively. The linearity in plot of  $1/(n_{ap} - 1)$  versus  $1/2kT$  indicates the existence of voltage deformation.

#### 4. Conclusions

The electrical, optical, and metal–semiconductor contact properties of the polyaniline prepared by emulsion have been investigated to obtain an organic semiconductor material. The polyaniline studied is an organic semiconductor material with direct optical band gap. The optical band gap of the polyaniline studied is smaller than that of polyaniline prepared by other methods. The ideality factor and barrier height of Ag/PANI/n-Si diode at room temperature were found to be 4.59 and 0.38 eV, respectively. The ideality factor and barrier height parameters of the diode changed with temperature. Ag/PANI/n-Si diode has a metal–insulator–semiconductor contact due to the

presence of an interfacial layer and effect of series resistance and interface inhomogeneity. The decrease in  $\phi_B$  and increase in the ideality factor with decreasing temperature were explained on the basis of a thermoionic mechanism with Gaussian distribution. The standard deviation, which is a measure of the barrier homogeneity, was found to be 0.14. This indicates the presence of interface inhomogeneities. It is concluded that the polyaniline prepared by emulsion polymerization is an organic semiconductor and the Ag/PANI/n-Si configuration shows a Schottky contact with metal–insulator–semiconductor configuration.

**Acknowledgment.** The study is supported by 2218-TUBİTAK-postdoctoral research scholarship program (807-2126).

#### References and Notes

- (1) Friend, R. H.; Gymer, R. W.; Holmes, A. B.; Burroughes, J. H.; Marks, R. N.; Taliani, C.; Bradley, D. D. C.; Dos Santos, D. A.; Bredas, J. L.; Logdlund, M.; Salaneck, W. R. *Nature* **1999**, *397*, 121.
- (2) Heeger, A. J. *Angew. Chem., Int. Ed.* **2001**, *40*, 2591.
- (3) Segura, J. L.; Martin, N. J. *Mater. Sci.* **2000**, *10*, 2403.
- (4) Kraft, A.; Grimsdale, A. C.; Holmes, A. B. *Angew. Chem., Int. Ed.* **1998**, *37*, 402.
- (5) Bernius, M. T.; Inbasekaran, M.; O'Brien, J.; Wu, W. S. *Adv. Mater.* **2000**, *12*, 1737.
- (6) Angelopoulos, M. *IBM J. Res. Dev.* **2001**, *45*, 57.
- (7) Nalwa, H. S., Ed. *Handbook of Organic Conductive Molecules and Polymers*; Wiley: Chichester, U.K., 1997.
- (8) Lux, F. *Polymer* **1994**, *34*, 2915.
- (9) Misra, S. C. K.; Chandra, S. Electronic applications of semiconducting polymers. *Indian J. Chem.* **1994**, *33A*, 583.
- (10) Gupta, R. K.; Singh, R. A. *Compos. Sci. Technol.* **2005**, *65*, 677.
- (11) Chung, S.-F.; Wen, T.-C.; Gopalan, A. *Mater. Sci. Eng. B* **2005**, *116*, 125.
- (12) Huang, L.-M.; Wen, T.-Ch.; Gopalan, A.; Fan, R. *Mater. Sci. Eng. B* **2003**, *104*, 88.
- (13) Kang, E. T.; Neoh, K. G.; Tan, K. L. *Prog. Polym. Sci.* **1998**, *23*, 211.
- (14) Masoud, M. S.; El-Enein, S. A.; El-Shereafy, E. *J. Therm. Anal.* **1991**, *37*, 365.
- (15) Tang, J.; Jing, X.; Wang, B.; Wang, F. *Synth. Met.* **1988**, *24*, 231.
- (16) Yakuphanoglu, F.; Erol, I. *Phys. B* **2004**, *352*, 378.
- (17) Davis, E. A.; Mott, N. F. *Philos. Mag.* **1970**, *22*, 903.
- (18) Mathai, C. J.; Saravanan, S.; Anantharaman, M. R.; Venkatachalam, S.; Jayalekshmi, S. *J. Phys. D: Appl. Phys.* **2002**, *35*, 2206.
- (19) Sajeev, S.; Mathai, C. J.; Saravanan, S.; Ashokan, R. R.; Venkatachalam, S.; Anantharaman, M. R. *Bull. Mater. Sci.* **2006**, *29*, 159.
- (20) Mukherjee, A. K.; Menon, R. *Pramana J. Phys.* **2002**, *58*, 233.
- (21) Sze, M. *Physics of Semiconductor Devices*; Wiley: New York, 1981.
- (22) Rhoderick, E. H. *Metal–Semiconductor Contacts*; Oxford University Press: London, 1978.
- (23) Liang, G.; Cui, T.; Varshney, K. *Solid-State Electron.* **2003**, *47*, 691.
- (24) Musa, I.; Eleon, W. *Jpn. J. Appl. Phys.* **1998**, *37*, 4288.
- (25) Lampert, M. A.; Mark, P. *Current Injection in Solids*; Academic Press: New York and London, 1970.
- (26) Gümüş, A.; Türüt, A.; Yalçın, N. *J. Appl. Phys.* **2002**, *91*, 245.
- (27) Werner, J. H.; Guttler, H. H. *J. Appl. Phys.* **1991**, *69*, 1522.
- (28) Lee, T. C.; Chen, T. P.; Fung, H. L.; Au, S.; Beling, C. D. *Phys. Stat. Sol. A* **1995**, *152*, 563.